Variable Voltage Battery Charging Capability DC-DC Converter with Fuzzy Controller

Latha.L.R, Roopa.C, M.Karthika

***Abstract*— Battery charger plays an important role in the battery and traction technology. Due to on-board type of charger it should be light in weight and should occupy less space as it should be on the vehicle all the time, so the smaller the better and of course, it is very important to minimize the cost of the charger. For a plug-in traction system, when the battery is charging from the grid, the vehicle should be parked. The traction system components are normally not engaged during the charging time, thus it is possible to reconfigure these components for the battery charger system. This concept presents the functionality of a commercialized fast charger for a lithium-ion battery. The device is intended to operate in a battery switch station, allowing an up-to 1-h recharge of a 25-kWh depleted battery, removed from a vehicle. The charger is designed as a dual-stage-controlled ac/dc converter. The input stage consists of a three-phase full-bridge diode rectifier combined with a reduced rating shunt active power filter. The input stage creates an uncontrolled pulsating dc bus while complying with the grid codes by regulating the total harmonic distortion and power factor according to the predetermined permissible limits. The output stage is formed by six interleaved groups of two parallel dc–dc converters, fed by the uncontrolled dc bus and performing the battery charging process. The charger is capable of operating in any of the three typical charging modes: constant current, constant voltage, and constant power. The proposed concept can be implemented with the Fuzzy based closed loop operation and verified through Matlab/simulink software.**

***Index Terms*— Battery charger, electric vehicle (EV), power converters, power quality**

I. INTRODUCTION

Numerous industrial applications have begun to require higher power apparatus in recent years [1].Power-electronic converters are becoming popular for various industrial drives applications. Electrification of the transportation industry is essential due to the improvements in higher fuel economy, better performance, and lower emissions [1]–[4]. In vehicular applications, power electronic dc/dc converters require high power flow capability with wide input range since the terminal voltage of energy storage devices varies with the state of charge (SoC) and load variations. In the case of an electric vehicle (EV), a dc/dc converter interfaces the energy storage device with the motor drive of the traction machine; i.e., the converter is placed between the battery and the high-voltage dc bus. The power-electronic technology plays a vital role in distributed generation and in integration of renewable energy sources into the electrical grid, and it is widely used and rapidly expanding as these applications become more integrated with the grid-based systems. The increasing number of renewable energy sources and distributed generators requires new strategies for the operation and management of the electricity grid in order to maintain or even to improve the power-supply reliability and quality. There are two common types of vehicle battery chargers. The onboard (often referred to as slow or low power) charger is located on board. The propulsion battery is recharged via the slow charger, plugged into a charging spot, while the vehicle is at parking lot [7]–[14]. The off board (so-called fast or high power) charger is located at the battery switch station (BSS). The battery must be removed from the vehicle to be recharged via the fast charger (FC).

The typical concept of EV includes urban driving only, where the full battery charge is sufficient for medium-range routes of 50–100 miles. Recharging is accomplished by plugging the car into charge spots placed at different city locations throughout the day and at driver's home during the night. Recently, a paradigm shift toward closing the gap between EV and conventional vehicles has occurred, forcing the infrastructure to support EV intercity driving as well. The following concept of BSS was developed: When out of charge, the EV battery can be replaced at a BSS, allowing nearly uninterrupted long range driving. The replacement process takes 2–4 min, similar to the duration of conventional re-fueling process. Actually, terrestrial applications of photovoltaic panels provide auxiliary means of power generation. Also, there are installations in locations where other means of electricity supply would be as costly as photovoltaic panels. However, it can be modified by splitting the three-phase rectifier into either two single-phase legs followed by two independent PFC converters or three single-phase Δ- or Y-connected stages. Apart from non linear loads, events like capacitor switching, motor starting and unusual faults could also inflict power quality (PQ) problems. PQ problem is defined as any manifested problem in voltage/current or leading to frequency deviations that result in failure or mal-operation of customer equipment. Alternatively, a more elegant approach employs a shunt-connected active power filter (APF) at the uncontrolled rectifier input, supplying the reactive current to the diode rectifier, thus achieving both near-unity PF and near-zero

Manuscript received Dec 12, 2015

Latha.L.R, Assistant Professor, Department of Electrical & Electronics Engineering, New Horizon College of Engineering, Bangalore, Karnataka, India

Roopa.C, Assistant Professor, Department of Electrical & Electronics Engineering, New Horizon College of Engineering, Bangalore, Karnataka,India

M.Karthika, Assistant Professor, Department of Electrical & Electronics Engineering,, New Horizon College of Engineering, Bangalore, Karnataka, India

total harmonic distortion (THD) by letting the utility to supply the active current only, which is in phase with the utility voltage and of the same shape. The During the past few decades, power industries have proved that the adverse impacts on the PQ can be mitigated or avoided by conventional means, and that techniques using fast controlled force commutated power electronics (PE) are even more effective. PQ compensators can be categorized into two main types. One is shunt connected compensation device that effectively eliminates harmonics. The other is the series connected device, which has an edge over the shunt type for correcting the distorted system side voltages and voltage sags caused by power transmission system faults [1], these power quality problems may cause abnormal operations of facilities or even trip protection devices. Hence, the maintenance and improvement of electric power quality has become an important scenario today.

This paper describes the development of a 50-kW commercial FC, employed in the first generation of BSS in Israel. Rather than presenting a novel topology, the main goal of this paper is to present a successful industrial application of well-known power electronics concepts. The charger employs a three-phase diode rectifier combined with three single-phase APFs as the input stage and twelve buck dc–dc converters, separated into six interleaved groups as the output stage. The power stage of the charger operates as a programmable voltage supply with controllable dynamic current limitation.

II. FC REQUIREMENTS

The FC, described in this paper, was designed to charge 355-V 70-A traction batteries formed by 96S2P connection of 3.7-V 35-A h lithium manganese spinal cells.

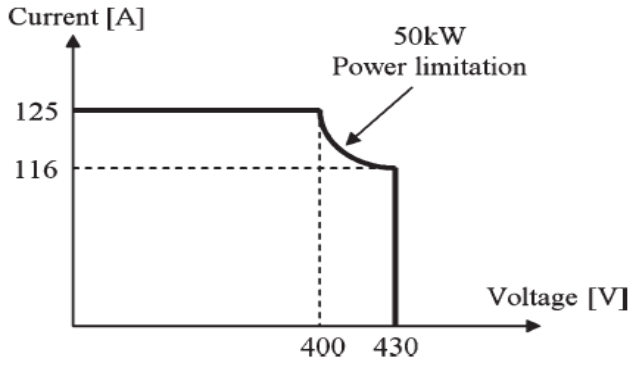

Fig.1. FC output performance envelope.

A. At Output Stage:

In order to charge such a battery, the FC must be able to operate in the full range of the possible battery voltages. In addition, power cable voltage drop should be taken into account. Hence, the maximum output voltage design requirement was set to 430 V. The maximum charging current was limited by the battery manufacturer to 125 A for safety reasons, leading to the charger output performance envelope requirement, shown in Fig. 1.

B. Input Stage:

The charger was designed to draw the power from 380- to 415-Vrms 50-Hz three-phase grids with neutral and protective earth connections. Since typical grid operators provide the ac power with 10% accuracy, the charger must be capable of functioning in the range of 342–457-Vrms input line voltages. The minimum consumer PF allowed by the Israel Electric Company in Israel is 0.92. Note that devices with active power correction usually operate with near-unity displacement factor (DF); therefore, the PF is affected mostly by the THD according to the following well-known relation:

$$\mathrm{PF} = \frac{\mathrm{DF}}{\sqrt{1+\mathrm{THD}^2}}.$$

In case the DF is kept near unity, the theoretical maximum allowed value of THD is 42.6%. However, since the rated input current exceeds 16 A, the charger emissions must comply with the IEC61000-3-4 standard, leading to the THD upper limit of 15%.

III. PROPOSED SYSTEM

The system-level block diagram of the proposed solution is presented in Fig. 2. On the signal level, the FC communicates with traction battery management system (BMS) and CMS terminal via CAN and Ethernet buses, respectively. The charger supports both master and slave mode charging. In the master mode, the charger performs either CC–CV of CP charging according to the CMS commands while monitoring the battery condition. In the slave mode, the battery manages the charging process by sending current/voltage/power requests to the charger. The CMS is the highest level management layer of a BSS, performing administration and billing tasks in addition to the ability of limiting or completely shutting down the FC fleet power in case of a safety issue or according to the utility grid operator request. In the charger under study, both communication protocols are realized by Zilog eZ80F91 microcontroller with the assistance of Grid connect RS232-CAN adaptor since eZ80F91 does not support the CAN bus directly. Zilog microcontroller is a bidirectional gateway between the CMS, battery BMS, and the Atmel At mega 128 microcontroller, which is in charge for the power management and monitoring of the charger power circuitry. The APF and buck control boards are independent and based on fully analog controllers. On the power level, there are low- and high-voltage links between the charger and the battery. The high-voltage link transfers the charging power, while the low-voltage (12 V) low-power link supplies power to the battery contactors. Note that the 12-V power supply, located inside the FC, is used to power both charger and battery contactors. The battery contactors are used to isolate the high-voltage power pack from the environment when the battery is not located in the vehicle or charging.

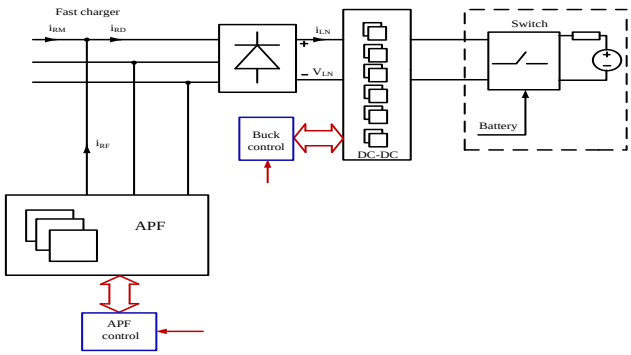

Fig.2. FC system-level block diagram.

Additional feature of the battery contactors is pre-charging of the vehicle inverter dc link capacitor upon battery connection. The charger contactors serve similar purposes since the charger dc–dc stage contains output capacitors which must be carefully pre-charged prior to the battery connection in order to prevent excessive inrush currents.

When a charging process is terminated, the charger output voltage is usually higher than 400 V. After the battery is disconnected, the output capacitors should be discharged to a low voltage because of safety reasons. This is accomplished by a bleeder circuit, discharging the output capacitors quickly below 50 V. The bleeder and the 12-V contactor power supply are both operated by the Atmega 128 microcontroller.

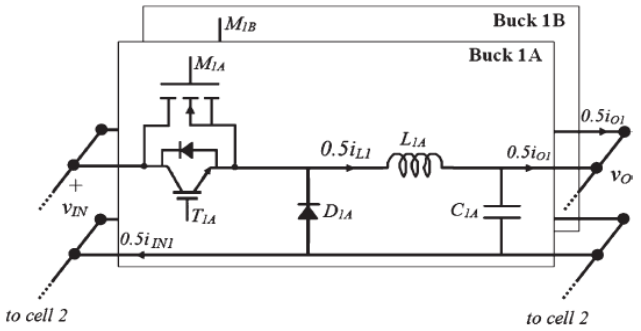

Fig.3. Buck cell structure

The dc–dc stage of the charger consists of six interleaved cells of two parallel 4.5-kVA buck converters [47], [48]. A single cell structure is shown in Fig. 3. The converters are of basic buck topology with an enhanced switch, consisting of a parallel connection of insulated gate bipolar transistor (IGBT) and MOSFET. A small delay between the turn-on and turnoff instants of the transistors allows relatively high switching frequency operation of 50 kHz and significant loss reduction. The input current of the dc–dc stage loads the diode bridge; hence, the current ripple is polluting the mains since the APF stage is unable to suppress high-frequency harmonics. Both ripple reduction and frequency increase lead to THD reduction and electromagnetic compatibility filter requirements loosening. The voltage at the input of the dc–dc stage is the rectified input voltage (for 400-Vrms grid). Since buck topology is employed at the output stage, the minimum value of the rectified voltage must be higher than the maximum output dc voltage in order to ensure undistorted operation. The minimum value of the rectified voltage is given by

$$V_{\mathrm{IN\,min}} = \frac{\sqrt{6} \cdot V_{\mathrm{rms}}}{2}$$

hence, the global minimum of the rectified voltage (neglecting the voltage drop of the diode bridge) is *VINmin* = 419 V for *V*rms = 342 V, and the requirement of maximum charge output voltage of 430 V cannot be met. As a result, the modification of the maximum output voltage requirement shown in Fig. 4 was proposed and accepted by the customer. It is worth noting that 410-V output is sufficient to charge the mentioned battery in most cases if the power cable is of a reasonable length and cross-sectional area since, during CV and CP charging stages, the current diminishes and cable voltage drop reduces proportionally with the current.

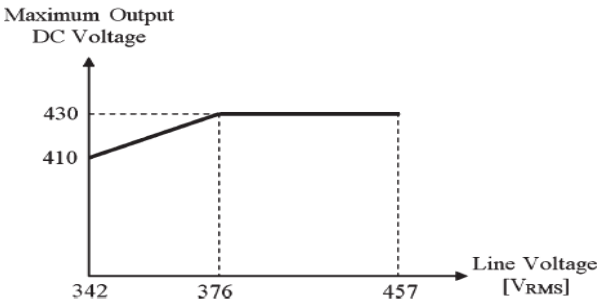

Fig.4. Modified maximum output voltage envelope.

The architecture of the dc–dc stage control circuitry is shown in Fig. 5. The analog control board receives from the Atmega 128 microcontroller reference voltage command in case of CV operation or reference current command in case of CC or CP operation, senses the real values of the appropriate voltage/ current, and creates PWM commands to switch drivers. The control algorithm has a conventional dual-loop structure, where the slow outer loop controls the charger output parameter (voltage or current, according to the operation mode) and the inner current mode control (CMC) loop controls the inductor currents of the individual converters to follow the outer loop generated reference. The interleaving is achieved by shifting the clocks used by CMC. The PWM signal, created by the current loop, is split into two time-delayed signals to the drivers of the combined switch transistors. Actual currents, voltages, and cell temperatures are continuously monitored by the Atmega 128 microcontroller, which can shut cells down in case of malfunction and perform corresponding output power derating. Control loop design and component selection issues are omitted for the sake of brevity.

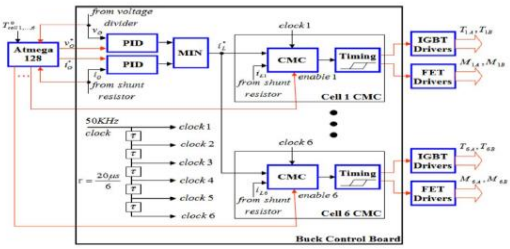

Fig.5. DC–DC stage control circuitry diagram.

The FC input stage consists of a three-phase diode rectifier and three single-phase APFs [50]. The reason of using three single-phase APFs instead of a single three-phase APF is the fact that a single-phase APF module was developed earlier by the company for another application and was found suitable for the first version of the FC. A three-phase APF employment is currently being developed for the future versions of the device. The diagram of the input stage phase *R* is shown in Fig. 6. The diode bridge is represented by a nonlinear current source *iRD*, which is supplied by both the mains and the APF. The main idea is forcing the APF to supply the reactive and harmonic content of the nonlinear current, leaving the mains to supply the fundamental harmonic only. The APF consists of a controlled full bridge with a dc bus capacitor (since it does not provide real power to the diode bridge), connected to the ac bus via an inductor. Although the diode bridge is represented by a current source, its actual behavior resembles a CP load since it drives a battery through dc–dc converter stage.

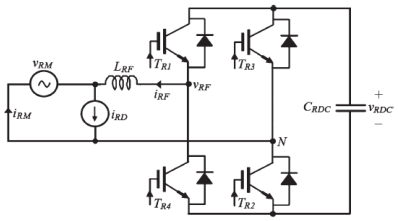

Fig.6. Input stage *R*-phase diagram.

In order to realize, the dc link voltage of the APF should be kept above the absolute maximum of the mains voltage because of the buck structure of the circuit. In addition, since there are internal switching and conduction losses in the APF, some amount of active current should be drawn by the filter from the mains to maintain the dc link voltage nearly constant. Moreover, there is a following trade off between the dc link voltage level and filter inductor: In order to prevent the switching frequency leakage, the inductor value should be as high as possible; however, a high inductor leads to the high frequency harmonics compensating ability deterioration since the dc link voltage increase is limited by the capacitor voltage rating. The trade-off values are eventually determined by PF and THD design requirements. If no solution is available satisfying all the constraints, an *LC* filter instead of a single inductor may be considered. However, in this case study, a single inductor solution turned out to be sufficient.

IV. FUZZY LOGIC CONTROLLER

A new language was developed to describe the fuzzy properties of reality, which are very difficult and sometime even impossible to be described using conventional methods. Fuzzy set theory has been widely used in the control area with some application to dc-to-dc converter system. A simple fuzzy logic control is built up by a group of rules based on the human knowledge of system behavior. Matlab/Simulink simulation model is built to study the dynamic behavior of dc-to-dc converter and performance of proposed controllers. Furthermore, design of fuzzy logic controller can provide desirable both small signal and large signal dynamic performance at same time, which is not possible with linear control technique. Thus, fuzzy logic controller has been potential ability to improve the robustness of dc-to-dc converters. The basic scheme of a fuzzy logic controller is shown in Fig 5 and consists of four principal components such as: a fuzzy fication interface, which converts input data into suitable linguistic values; a knowledge base, which consists of a data base with the necessary linguistic definitions and the control rule set; a decision-making logic which, simulating a human decision process, infer the fuzzy control action from the knowledge of the control rules and linguistic variable definitions; a de-fuzzification interface which yields non fuzzy control action from an inferred fuzzy control action [10].

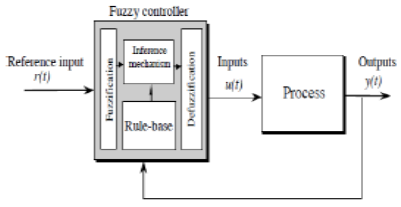

Fig.7. General Structure of the fuzzy logic controller on closed-loop system

The fuzzy control systems are based on expert knowledge that converts the human linguistic concepts into an automatic control strategy without any complicated mathematical model [10]. Simulation is performed in buck converter to verify the proposed fuzzy logic controllers.

V. MATLAB MODELING AND SIMULATION RESULTS

Here simulation is carried out in three different conditions, in that 1. Proposed Battery Charger with DC-DC Converter with Power Factor Correction Scheme, 2. Proposed Battery Charger with DC-DC Converter closed loop operation with fuzzy controller.

Case 1: Proposed Battery Charger with DC-DC Converter with power quality improvement

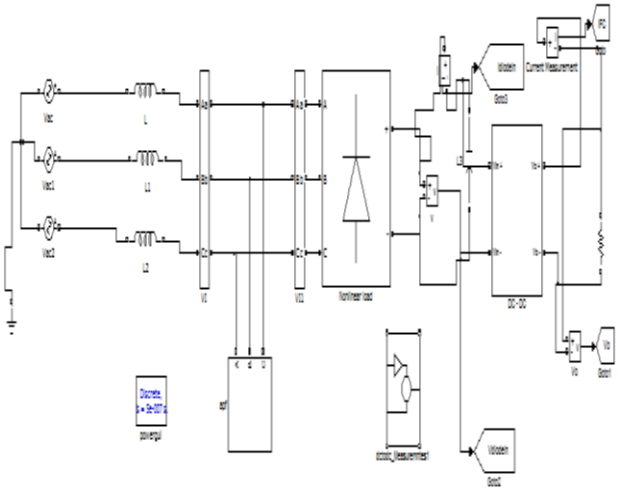

Fig.8. Matlab/Simulink Model of Proposed Battery charger with DC-DC Converter.

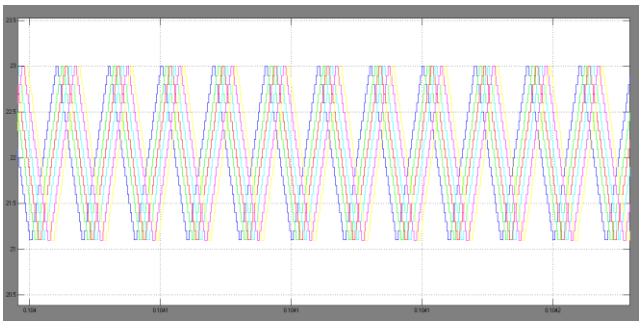

Fig.9. Individual buck cell inductor currents.

Fig.9. shows the Individual buck cell inductor currents of Proposed Battery charger with DC-DC Converter.

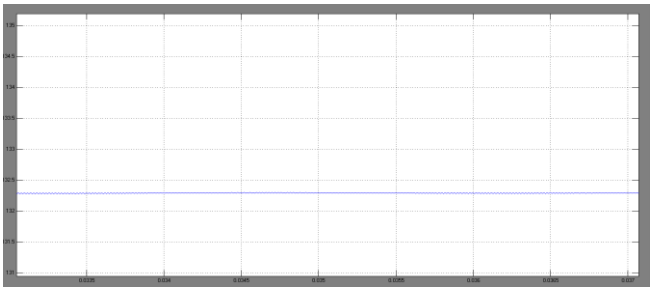

Fig.10. FC output current after capacitor filter.

Fig.10. shows the FC output current after capacitor filter of Proposed Battery charger with DC-DC Converter.

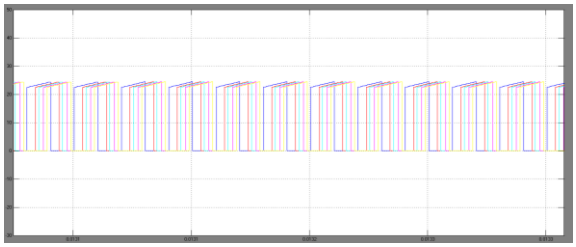

Fig.11 Individual buck cell improved input currents.

Fig.11. Individual buck cell Improved input currents of Proposed Battery charger with DC-DC Converter.

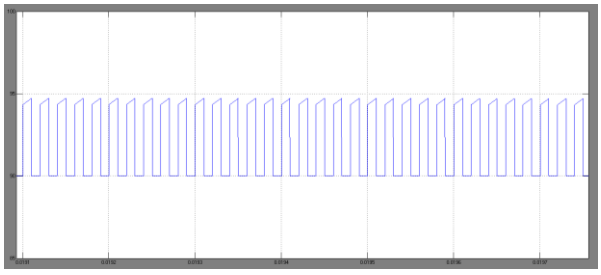

Fig.12 DC–DC stage input current.

Fig.12. shows the DC–DC stage improved input current of Proposed Battery charger with DC-DC Converter.

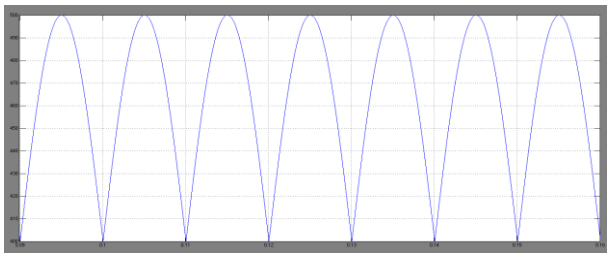

Fig.13.Rectified voltage at the dc–dc stage input.

Fig.13. shows the Rectified voltage at the dc–dc stage input of Proposed Battery charger with DC-DC Converter.

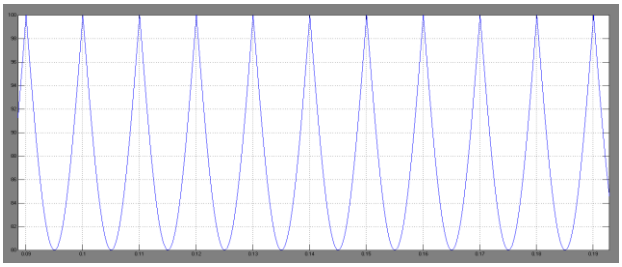

Fig.14. Worst case bridge rectifier output current.

Fig.14. shows the Worst case bridge rectifier output current of Proposed Battery charger with DC-DC Converter.

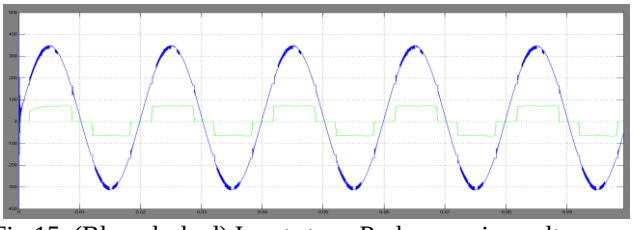

Fig.15. (Blue; dashed) Input stage *R*-phase mains voltage and (green; solid) Diode Bridge current.

Fig.15 shows the Input stage *R*-phase mains voltage and Diode Bridge current.

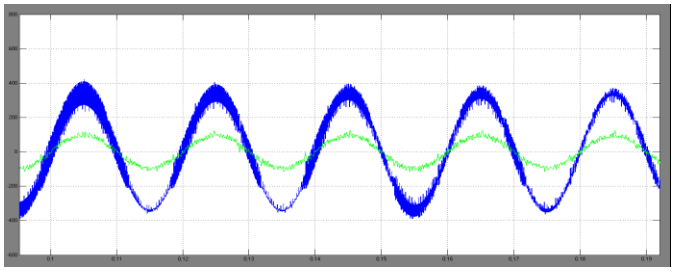

Fig.16. Input stage performance (phase *R*): (Upper) (Blue; dashed) Mains voltage and (green; solid) current.

Fig.16. shows the Supply Voltage & Current of Proposed Battery charger with DC-DC Converter.

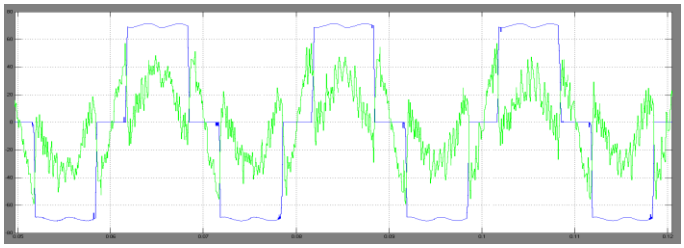

Fig.17. (blue; dashed) diode bridge and (green; solid) APF currents.

Fig.17 shows Input stage performance of Diode Bridge and APF currents.

Case 2: Proposed Battery Charger with DC-DC Converter performed closed loop operation with Fuzzy controller

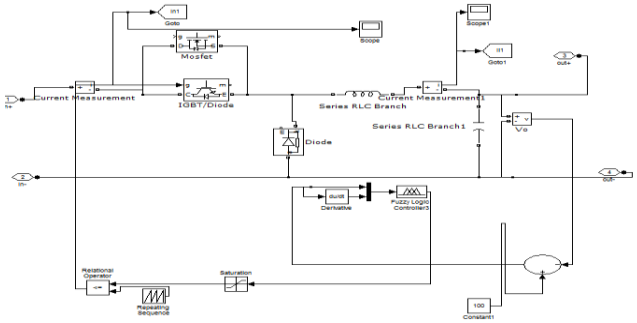

Fig.18. Matlab/Simulink Model closed loop operation with fuzzy controller.

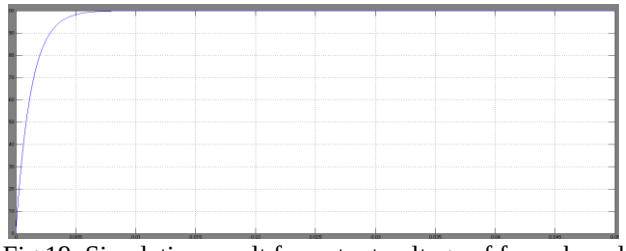

Fig.19. Simulation result for output voltage of fuzzy based closed loop dc-dc converter.

CONCLUSION

Closed loop fuzzy systems offer better performance compared to open loop system. The device is capable of supplying up to 50-kW charging power to any battery, operating in 240–430-V voltage range in CC, voltage, or power mode. The charger topology may be referred to as a two stage controlled rectifier. The input stage consists of a

three phase full-bridge rectifier combined with a reduced rating APF (three single-stage power filters are actually employed). The input stage creates an uncontrolled dc bus while complying with the grid codes by keeping the THD and PF within the permissible limits. The output stage is formed by six interleaved groups of two dc–dc converters, reducing the input and output current ripples. Two independent control boards are employed: active filters control circuitry and the dc–dc control circuitry. The former is operated according to the predetermined grid interfacing behavior, while the operation of the latter is dictated either by pre-programmed charging sequence or by the requests from the BMS. From fig.19 and fig.21 we can conclude that after using fuzzy controller the settling time of dc voltage is 0.025 sec. The designed device performance is shown to comply with main design requirements, and extended simulation results are presented.

REFERENCES

[1] Battery Charger for Electric Vehicle Traction Battery Switch Station A. Kuperman, *Member, IEEE*, U. Levy, J. Goren, A. Zafransky, and A. Savernin, IEEE TRANSACTIONS ON INDUSTRIAL ELECTRONICS, VOL. 60, NO. 12, DECEMBER 2013

[2] B. Kennedy, D. Patterson, and S. Camilleri, "Use of lithium-ion batteries in electric vehicles," *J. Power Sources*, vol. 90, no. 2, pp. 156–162, Oct. 2000.

[3] R. Gitzendanner, F. Puglia, C. Martin, D. Carmen, E. Jones, and S. Eaves, "High power and high energy lithium-ion batteries for underwater vehicles," *J. Power Sources*, vol. 136, no. 2, pp. 416–418, Oct. 2004.

[4] G.-C. Hsieh, L.-R. Chen, and K.-S. Huang, "Fuzzy controlled Li-ion battery charge system with active state-of-charge controller," *IEEE Trans. Ind. Electron.*, vol. 48, no. 3, pp. 585–593, Jun. 2001.

[5] M. Chen and G. Rincon-Mora, "Accurate, compact, and power-efficient Li-ion battery charger circuit," *IEEE Trans. Circuits Syst. II, Exp. Briefs*, vol. 53, no. 11, pp. 1180–1184, Nov. 2006.

[6] K. Tsang and W. Chan, "A simple and low-cost charger for lithium-ion batteries," *J. Power Sources*, vol. 191, no. 2, pp. 633–635, Jun. 2009.

[7] J.-J. Chen, F.-C. Yang, C.-C. Lai, Y.-S. Hwang, and R.-G. Lee, "A high efficiency multimode Li-ion battery charger with variable current source and controlling previous stage supply voltage," *IEEE Trans. Ind. Electron.*,vol. 56, no. 7, pp. 2469–2478, Jul. 2009.

[8] D. Thimmesch, "An SCR inverter with an integral battery charger for electric vehicles," *IEEE Trans. Ind. Appl.*, vol. IA-21, no. 4, pp. 1023– 1029, Jul. 1985.

[9] J. Bendien, G. Fregien, and J. vanWyk, "High-efficiency on-board battery charger with transformer isolation, sinusoidal input current and maximum power factor," *Proc. Inst. Elect. Eng.—Elect. Power Appl.*, vol. 133, no. 4, pp. 197–204, Jul. 1986.

[10] S.-K. Sul and S.-J. Lee, "An integral battery charger for four-wheel drive electric vehicle," *IEEE Trans. Ind. Appl.*, vol. 31, no. 5, pp. 1096–1099, Sep./Oct. 1995.

[11] B. Masserant and T. Stuart, "A maximum power transfer battery charger for electric vehicles," *IEEE Trans. Aerosp. Electron. Syst.*, vol. 33, no. 3, pp. 930–938, Jul. 1997.